Hindawi
Scientific Programming
Volume 2023, Article ID 9867242, 1 page
https://doi.org/10.1155/2023/9867242

Retraction

Retracted: Application and Performance Discussion of Fiber-Reinforced Composite Materials in Sports Equipment Based on Image Processing Technology

Scientific Programming

Received 1 August 2023; Accepted 1 August 2023; Published 2 August 2023

This article has been retracted by Hindawi following an investigation undertaken by the publisher [1]. This investigation has uncovered evidence of one or more of the following indicators of systematic manipulation of the publication process:

(1) Discrepancies in scope
(2) Discrepancies in the description of the research reported
(3) Discrepancies between the availability of data and the research described
(4) Inappropriate citations
(5) Incoherent, meaningless and/or irrelevant content included in the article
(6) Peer-review manipulation

The presence of these indicators undermines our confidence in the integrity of the article's content and we cannot, therefore, vouch for its reliability. Please note that this notice is intended solely to alert readers that the content of this article is unreliable. We have not investigated whether authors were aware of or involved in the systematic manipulation of the publication process.

Wiley and Hindawi regrets that the usual quality checks did not identify these issues before publication and have since put additional measures in place to safeguard research integrity.

We wish to credit our own Research Integrity and Research Publishing teams and anonymous and named external researchers and research integrity experts for contributing to this investigation.

The corresponding author, as the representative of all authors, has been given the opportunity to register their agreement or disagreement to this retraction. We have kept a record of any response received.

References

[1] E. Liu, "Application and Performance Discussion of Fiber-Reinforced Composite Materials in Sports Equipment Based on Image Processing Technology," *Scientific Programming*, vol. 2022, Article ID 6879601, 12 pages, 2022.

Hindawi
Scientific Programming
Volume 2022, Article ID 6879601, 12 pages
https://doi.org/10.1155/2022/6879601

Research Article

Application and Performance Discussion of Fiber-Reinforced Composite Materials in Sports Equipment Based on Image Processing Technology

Erwei Liu

Students Affairs Department, Chongqing Vocational College of Transportation, Jiangjin 402247, Chongqing, China

Correspondence should be addressed to Erwei Liu; liuerwei@cqjy.edu.cn

Received 30 June 2022; Revised 12 August 2022; Accepted 25 August 2022; Published 24 September 2022

Academic Editor: Juan Vicente Capella Hernandez

Fiber reinforced composites can meet the needs of lightweight, heavy load, long-span, high strength, and modern structures and work under strict conditions. Therefore, it is widely used in various fields. Sports equipment generally cannot meet the requirements of high-strength use, so there is an urgent need for new fiber materials to make these instruments. Aiming at improving the efficiency of measurement and the reliability of measurement results, this paper studies the quantitative characterization method of the microstructure of short fiber reinforced composites. The swept-frequency OCT system is a newly developed high-resolution biomedical imaging system. The method of this paper is to study the performance parameters of swept frequency OCT system, deduce the application of image processing technology in fiber material detection, and then study the detection of residual strength and residual stiffness of composites, so as to obtain a composite material detection method that can be popularized. On this basis, image processing and performance analysis of the composites were carried out, and the composites were tested. And the prospect of application in this field has been analyzed. The experimental results show that better fiber length can be obtained by this method, and the maximum relative error is only 4.5%, thus ensuring the accurate determination of fiber length. Calculations were carried out using the experimental data, and the results showed that the performance of the sports product increased from 15.4% to 48.6% with the graphite-rubber composite. Using this material can improve the comprehensive performance of sports equipment by 2.1%~4.5%.

1. Introduction

1.1. Background. The discovery and utilization of all important material materials in history will bring significant changes to human production and living standards and social productivity. Material is the material basis for human survival and development and plays an important role in human society. Juxtaposed with energy and information, it is known as the three pillars of modern human society. After the 20th century, due to the rapid development of science and technology, in order to meet the human demand for new products of high-performance materials, the role of traditional materials is dwarfed, so multistructure composites are produced. High-performance structural materials refer to those materials with special properties such as high strength, high toughness, high-temperature resistance, wear resistance, and corrosion resistance. Compared with single polymer materials or other traditional materials, fiber-reinforced composites have many advantages, such as large elasticity, high specific heat capacity, simple molding process, good fatigue resistance, good shock absorption, good overload safety, and strong functionality, which makes them the most widely used and widely used composite materials at present. Measuring the length and orientation of fibers in short fiber reinforced composites plays a very important role in analyzing the macro mechanical properties of materials. This paper discusses the application and performance of fiber-reinforced composite materials in sports equipment based on image processing technology, in order to make certain contributions to fiber-reinforced composite materials.

1.2. Significance. This study aims to improve the efficiency and reliability of the quantitative characterization of short fiber reinforced composite materials and explore a simple and reliable method to measure the fiber length and orientation distribution in short fiber reinforced composite materials, thereby reducing the difficulty and strength of characterization. The quantitative characterization of microstructure promotes the effective development of the quantitative relationship between microstructure and macroscopic properties. It is hoped that the research in this article can contribute to the development of quantitative research on the microstructure of short fiber reinforced composite materials and improve the movement performance of the equipment.

1.3. Related Work. The image processing technology is more and more widely used in the analysis of fiber-reinforced composites. Jia and Zhang introduced Hadoop-based image resource storage technology to improve the reading speed of image resources, and then uses a random forest algorithm to mine image recognition digital information and recommend the most appropriate online resources. He introduced augmented reality technology to enhance the immersion and interactivity of online education, so that image processing technology can develop appropriate interactive functions according to different scenes, enhance the immersion and participation of online teaching, comprehensively improve the quality of teaching and learning, and provide technical support for the improvement of online learning. However, this image processing technology focuses on information output, the lack of image analysis, and learning [1]. Oho et al. propose an efficient and fast scanning method combined with digital image processing technology to replace the traditional slow scanning mode as the standard acquisition model of general scanning electron microscope. The scanning electron microscope image obtained by using the proposed method has the same quality as the slow scanning image in terms of sharpness and noise, and can suppress the adverse effect of charging under a full vacuum. However, this technology uses the inverse filter based on the frequency characteristics of TV scanned images to properly compensate for the image quality. It is a fuzzy image integration technology, which has no obvious effect on noise suppression, and its position is not robust to noise [2]. Gu et al. analyzed that behavior recognition based on image recognition is an active research field in computer vision. He believes that with the modernization of animal husbandry, innovative technologies such as machine vision and artificial intelligence are gradually applied to biological monitoring, which can realize biological real-time abnormal behavior and biological behavior analysis. Behavior analysis includes biological image sequence, viewfinder, target classification, anomaly detection, and behavior recognition. His research is based on individual behavior image recognition and deduces the analysis function of image recognition. However, his research needs to establish a large number of biological action databases to realize comparative analysis. It is difficult to popularize this technology [3]. Elhousari et al. believe that reinforced thermoplastic composites have excellent corrosion resistance, high specific strength, high impact toughness, high specific stiffness, recyclability, cost-effectiveness and design flexibility, and have considerable advantages in structural and industrial applications. In order to obtain better mechanical properties, reduce the total cost, and enhance the performance of polypropylene composites, he proposed that recycled rubber powder be used as a low-cost additive for polypropylene composites/glass fiber composites. However, his improved method of mixing polypropylene composites and glass fibers with different weight ratios has higher requirements for the injection molding machine, consumes more energy in the production process, and has no obvious cost advantage [4]. Yamamoto and Okabe proposed an accurate tensile strength prediction method for fiber-reinforced composites. He believes that the accurate tensile strength prediction of unidirectional carbon fiber reinforced plastic composites (UD) needs to roughly determine the stress concentration on the remaining fibers around the fiber fracture point. The stress concentrated on the surface of the intact fiber is determined by a double fiber fragment test combined with spring element model simulation. However, carbon fiber is a very special fiber composite, and its characteristics are more distinctive than other materials, so its prediction method is not universal [5]. Hamanaka et al. investigated the correlation between the fiber orientation distribution along the thickness direction and mechanical anisotropy in injection molded products using short fiber-reinforced thermoplastic resin. Then, the fiber orientation distribution near the center of the plate was observed by X-ray computed tomography, and the fiber orientation distribution along the thickness was quantified by a fiber orientation tensor. Then cut the sample from the plate along the machine and transverse direction, and conduct the three-point bending test. Finally, the evaluation results of fiber orientation distribution and mechanical anisotropy are compared. His method is to analyze the material composition, but this analysis is mechanically repeated and can be completed by computer technology, which will be faster and more accurate [6]. Matsuwaka and Latzka analyzed that with the increasing popularity of adaptive sports, the research on improving sports equipment to prevent athletes from facing injury has become more and more important. His survey found that wheelchair basketball, football, tennis, track and field, swimming and football were the most frequently studied in recent years. Injuries vary from sport to sport due to different levels of exposure, limbs used, and athlete injuries. Changes in equipment and technological advances, especially in wheelchairs and amputations, have improved the level of competition and reduced the injury rate. However, he studied the replacement of equipment and neglected to start with equipment manufacturing materials [7]. Starting from the structural materials of sports equipment, Feng and Wang raised the issue of comfort, and then elaborated on the polymer composite materials, and made a case design and analysis of the applicability of polymer composite materials in sports equipment [8]. Jahangir et al. have experimentally investigated the compressive performance of short concrete

columns with square cross-sections confined by steel fiber reinforced polymer and grouting composites SRP and SRG composites [9]. The application of composite materials in aircraft structure is a hot research topic at present. Li et al. mainly discussed the optimal design of the composite wing structure of the DF-2 light sport aircraft [10].

1.4. Innovation Points. The innovations of this study are as follows: (1) Through the hybrid compounding of organic fibers and inorganic fibers, the polypropylene/ethylene vinyl acetate matrix is reinforced and modified to make composite fiber materials with strong comprehensive properties. (2) The experiment and performance analysis of composite fiber image processing were carried out.

2. Image Processing Technology and Composite Strength Detection Method

2.1. Sweep Frequency OCT System Performance Parameters. In order to achieve the purpose of rapid imaging of scanning OCT system, researchers at home and abroad have studied the improvement of OCT system structure and light source while optimizing the postprocessing algorithm of OCT Research Institute. OCT is optical coherence tomography, which is a non-invasive, noncontact, cross-sectional scan of the retina's fine structure in vivo. This study briefly introduces the classification of OCT systems and the investigation of speckle noise elimination at home and abroad. By analyzing the performance parameters and noise sources of the scanning optical coherence tomography system, the noise model of the system is established and the noise simulation is carried out. OCT is one of the most promising new tomographic imaging technologies that has developed rapidly in recent years, especially in biological tissue biopsy and imaging, which has attractive application prospects. In this study, a fast image noise elimination algorithm based on wavelet packet decomposition and least square error filtering is designed. Compared with various OCT image noise elimination methods, the effectiveness of the algorithm is verified. OCT is a non-contact, high-resolution tomographic and biological microscope imaging device. It can be used for in vivo viewing, axial tomography, and measurement of posterior ocular structures, and is particularly useful as a diagnostic device to aid in the detection and management of eye diseases. The schematic diagram of material manufacturing image processing technology is shown in Figure 1.

According to the theory of frequency scanning signal-to-noise ratio, the ratio of signal-to-noise photocurrent to the intensity of noise photocurrent after Fourier transform is the signal-to-noise ratio of the system. Assuming that i_a can represent the signal photocurrent, the signal power f_a^2 is the intensity of the signal photocurrent after Fourier transform, that is, the intensity f_b^2 of the signal photocurrent, in which the noise photocurrent $i_s i_b$. The signal-to-noise ratio of scanning optical coherence tomography systems can be expressed by the following formula:

$$SNR = \frac{f_a^2}{f_b^2}. \tag{1}$$

If it is assumed that the reflectivity on the reflective interface is fixed, when the instantaneous linewidth of the scanning light source in the scanning OCT system is small enough, the signal photocurrent i_a is followed by the noise photocurrent i_b. If the reflectivity on the reflective interface x_0 is fixed, the coherence function of the light source can be approximately 1. In addition, the signal photocurrent and time formula can be expressed by the following formula:

$$i_a(t) = \frac{2nq}{h\nu}\sqrt{W_a W_r}\cos\ (2K(t)x_0). \tag{2}$$

Here, $h\nu$ is the photon energy, q is the electron quantity, n is the quantum efficiency coefficient, W_a is the optical power reaching the detector on a single-layer reflection interface x_0, and W_r is the optical power returning to the detector from the reference arm [11]. At this time, there is $W_a = r^2 W_0$, and r is the reflection coefficient of the sample. At this time, the average noise power (t) of the system can be expressed by the following formula:

$$i_b^2(t) = \left[i_t^2(t) + \frac{2nq^2}{h\nu}(W_a + W_r) + \frac{nq^2}{h\nu}RIN(W_a + W_r)^2\right]BW. \tag{3}$$

The noise of the system is caused by $(2nq^2/h\nu)(W_a + W_r)$ indicates that the high-temperature noise of the system is represented by $i_t^2(t)$ in the formula, and the relative intensity noise of the swept frequency light source is represented by $(nq^2/h\nu)\mathrm{RIN}(W_a + W_r)^2$. H_z^{-1} is the common unit of three kinds of noise, the bandwidth of the photodetector is expressed by BW, and the Fourier conversion method of signal photocurrent can be expressed by an (4). In this formula, the signal photocurrent at the single-layer reflection interface z_l is expressed as i_a.

$$f_s(z_l) = \sum_{b=0}^{N_a - 1} i(k_b)\exp\left(\frac{-2j\pi bl}{N_a}\right). \tag{4}$$

In the above formula, N A is the number of sampling points in each cycle of the system, and the signal photocurrent is (kb). According to Pascal's theorem: $\sum f^2 = N_a \sum i^2$, formula (5) is the signal photocurrent i (kb) after square conversion processing by the Fourier conversion method.

$$\left|f_a^2\right| = \left(\frac{N_a^2}{2}\right)i_a^2. \tag{5}$$

At this time, the signal-to-noise ratio of the system can be defined as follows:

$$\mathrm{SNR} = \frac{N_a}{2}\frac{i_a^2}{i_b^2}. \tag{6}$$

It can be seen from the formula that the SNR of the time-domain OCT system is i_a^2/i_b^2. Therefore, the signal-to-noise ratio of the frequency scanning OCT system is twice higher as that of time-domain OCT system. Compared with speckle

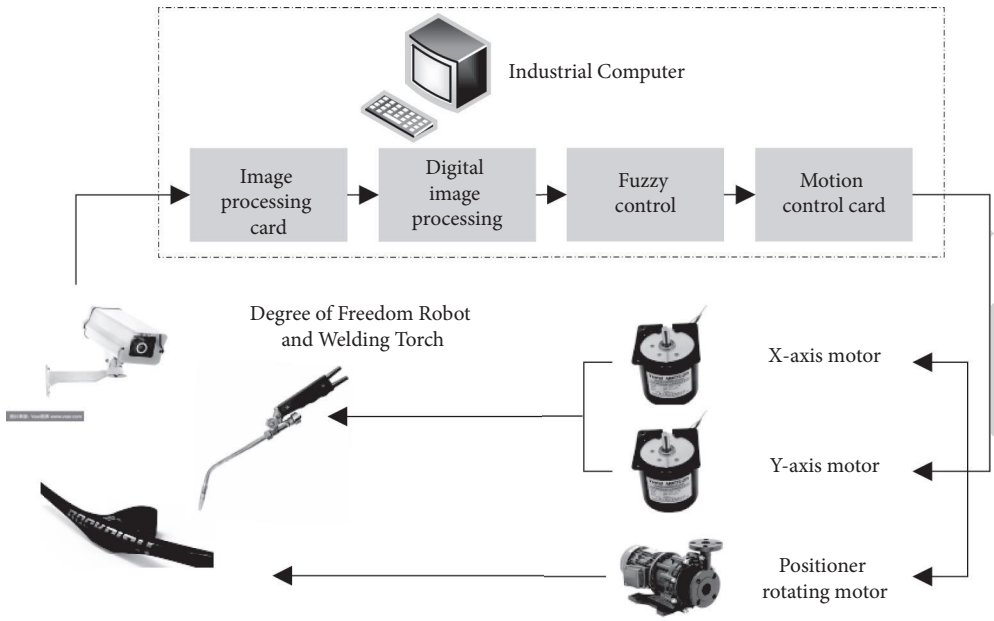

Figure 1: Visual tracking processing technology for composite manufacturing.

noise, the other two kinds of noise can be ignored in scanning OCT systems. When $W_a < W_r$, the SNR of the scanning OCT system is represented by expression as follows:

$$\mathrm{SNR} = \frac{nW_a}{hvf_a}. \tag{7}$$

In the above equation, fa is the scanning frequency of line a, that is, the scanning frequency of the scanning light source [12]. Therefore, if the reflected signal of the detected object is not too strong, the scanning speed of the swept OCT system is relatively low, but the reflected signal can be detected [13]. OCT is a new optical diagnostic technique that enables noncontact, noninvasive tomographic imaging of the microscopic structure of living ocular tissue.

2.2. Residual Strength of Composites. Many fiber-reinforced composites predict fatigue life based on residual strength, so the residual strength of fiber-reinforced composites is particularly important under fatigue strength [14]. Composite material is a new material that people use advanced material preparation technology to optimize the combination of material components with different properties. All kinds of damage are accompanied by repeated loading process, and its strength decreases. Due to reduced performance, the degree of material damage can be accurately visualized [13].

Different from metal materials, there is no reliable method to predict the service life of composites. When the number of cycles reaches a critical point, if the number of cycles continues to increase, the tendency of residual strength decreases sharply, and poor fracture may occur at this stage [2]. The matrix materials of composite materials are divided into two categories: metal and non-metal [15, 16]. The failure mode does not depend on the expansion of the main crack and depends on the strength distribution of the structure [17]. Figure 2 shows the variation curve of the residual strength of the composite with the increase in the number of cycles.

It is a general method to predict fatigue life by residual strength. When the residual strength reaches the maximum external stress, the material will be damaged and destroyed [17]. Load time, stress ratio, and load size are mainly used to reduce the strength of composites.

$$\theta(n) = f(n, \theta_{\max}, R). \tag{8}$$

In formula (8), $\theta(n)$ Is the residual strength of the composite after n fatigue loads. $\theta_{\max}$ is the maximum value under the maximum fatigue load, and R is the stress ratio of the fatigue load at this time, $R = \theta_{\max}/\theta_{\min}$, two boundary conditions must be met. When $n = 0$, that is, when no load is applied, $\theta(n) = \theta_{\mathrm{ult}}$, θ_{ult} represents the static strength in the load direction. The residual strength of glass fiber composites was analyzed by experiments [18]. It has been proposed that the residual strength of composites decreases linearly with the increase of the number of cycles. The model is given as follows:

$$\frac{R(n) - \theta_{\max}}{R(0) - \theta_{\max}} = 1 - \frac{n}{N_f}, \tag{9}$$

where $f = n/N$, $R(0)$ is the initial strength and $R(n)$ is the residual strength after N cycles. In the process of continuous loading, the fatigue time is superimposed, and the residual strength changes according to the rule of exponential function [19]. Therefore, the residual strength model proposed in this paper is exponential and is given as follows:

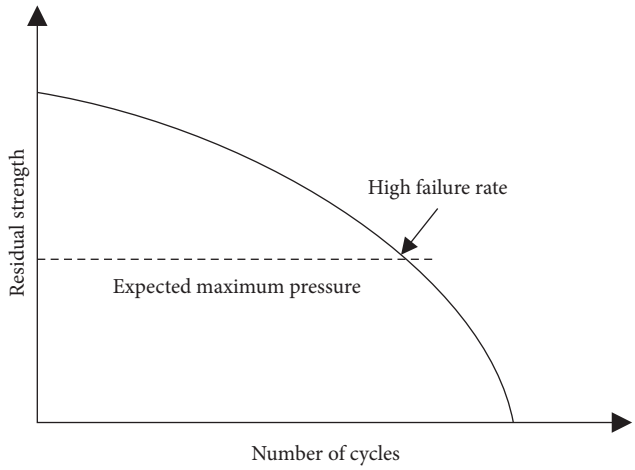

Figure 2: Residual strength variation curve.

$$\frac{R(n)-\theta_{\max}^{m}}{R(0)-\theta_{\max}^{m}}=1-\left(\frac{n}{N_i}\right)^{q}. \tag{10}$$

The parameter q is determined by experiment. Then, on this basis, this paper assumes that the residual strength attenuation rate at the initial time is 0, $R(n)/n=0$, and generalizes it. The model is given as follows:

$$\partial[R(n)]=\partial[R(0)]-\{\partial[R(0)]-\partial\theta_{\max}\}\left(\frac{\log n}{\log N}\right). \tag{11}$$

The model is shown below. Because ∂ can only be determined by many experiments, and the cost of engineering application is very high. Therefore, this paper summarizes the damage propagation rules of fiber-reinforced composites under fatigue load. The residual strength model proposed in this paper has strong adaptability, indicating that the residual strength is consistent with the damaging trend [20]. The model is shown as follows:

$$R(n)=R(0)-(R_0-\theta)+\theta\left[\frac{\sin bk\cos(b-a)}{\sin b\cos(bk-a)}\right], \tag{12}$$

where $k=n/N$, a and b are parameter values determined by experiment. In addition, as shown in equation (13), a power-law degradation form of fatigue damage is proposed in this paper.

$$R(n,\theta,k)=\left[1-N^{b}\right]^{1/a}(R_0-\theta)+\theta. \tag{13}$$

Among them, a and b are the experimental fitting coefficients, which are independent of the stress state, but only one residual strength can be measured for a test piece. This paper points out that when the damage state of the sample is characterized by residual strength, it is difficult to compare, and the two do not necessarily correspond. In the continuous process, the damage always changes, but in the initial stage, the strength decreases slightly and then decreases sharply [21]. Therefore, predicting the life of structures with residual strength is not a very ideal method.

2.3. Residual Stiffness of Composites. Due to the action of repeated load, the stiffness of the composite can be continuously measured during damage accumulation and expansion and does not affect the properties of the material [22]. Therefore, rigidity is a test parameter that can well reflect the properties of composites, and composites have anisotropic properties. In order to fully describe the characteristics of rigidity, at least four quantities need to be considered, namely E_x, E_y, G_{xy}, and V_{xy}. Because the experimental measurement method is difficult, we mainly study the change of material rigidity in the load direction. There are many definitions of stiffness for different descriptions in academia [23]. As shown in Figure 3, many scholars analyze it from the perspective of experience, theory, or a combination of the two.

In the fiber-reinforced composite laminate, the stiffness morphology is different at different stages. Figure 4 shows a typical stiffness reduction curve.

In the initial stage, the first stage damage occurs, and the main reason for the sharp decline of rigidity is that there are many cracks in the matrix, and the second stage tends to be stable [24]. The main reason is that the crack of the matrix is not enough to propagate to the fiber, and the stress at the tip of the matrix is not enough to damage the fiber. When the load increases, the rigidity decreases slowly. In the third stage, a large number of cracks accumulate, the fiber strength decreases than the stress at the crack tip, the fiber is damaged, and the rigidity decreases sharply [25]. After comparing the experimental results, a one-dimensional shear delay model is proposed, and the relationship between crack density and stiffness reduction is studied. However, the shear stress is transmitted between the transverse and longitudinal layers, and the shear force between adjacent layers is considered not to be transmitted.

Because the change of stiffness can be used to describe the fatigue damage of materials, many scholars at home and abroad say that the cumulative damage of composites is in the form of stiffness attenuation [26, 27]. Through comparative experimental research, the corresponding stiffness reduction model is proposed.

$$\frac{E(n)}{E(0)}=1-\left(1-\frac{E_n}{E_0}\right)\frac{n}{N_f}. \tag{14}$$

The stiffness value of aperiodic material is represented by $E(0)$, the residual stiffness value after N cycles is represented by $E(n)$, and the corresponding fatigue life value is represented by N_f. Formula (15) represents the relationship between residual strength, applied load, and cycle time.

$$E(n)=E(0)\left[1-K\left(\frac{\theta_{\max}}{E(0)}\right)^{a}n^{b}\right], \tag{15}$$

where k, a, and b are obtained through experiments, $\theta_{\max}$ is the maximum stress value under fatigue load. After N cycles of load, the remaining strength control can be expressed by the following formula.

$$E(n)=E(0)\left[1-Wn^{v}\right]. \tag{16}$$

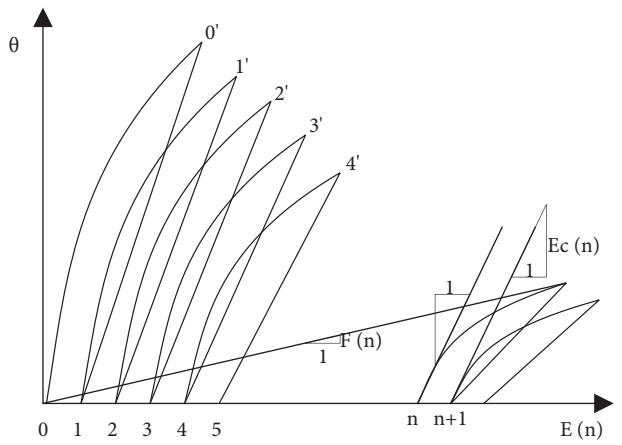

Figure 3: Definition of stiffness.

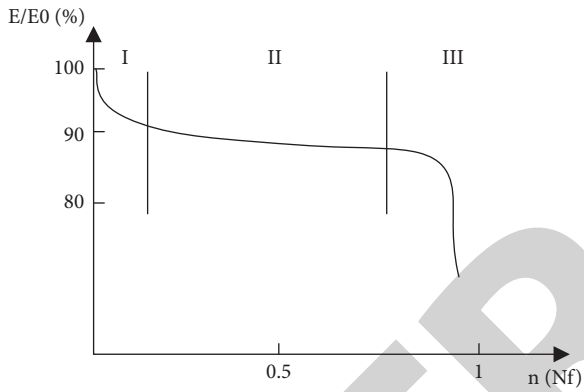

Figure 4: Stiffness degradation curve.

In the equation, the initial elastic parameter is e (0), $W = a_1 + a_2 v$, the stress level has a linear relationship with the average value v. Next, this paper studies the rigidity deterioration law of laminated plates with the same characteristics and carries out a tensile fatigue test on the test piece [28, 29]. Since the deterioration effect is considered to be almost independent of the magnitude of the stress level, a deterioration model under different stress levels is proposed as follows:

$$E(n) = E(0)\left[S\left(\frac{n}{N_f}\right) + 1\right], \tag{17}$$

where s is the parameter measured experimentally. Under the action of fatigue load, the corresponding deterioration model is established according to the rigid attenuation law of laminated materials, and the statistical distribution formula is derived as follows:

$$E(n) = E(0) * \exp\left[-S\left(\frac{n}{N_f}\right)^{b+c\theta}\right]. \tag{18}$$

S and C are related to load frequency, stress level and stress ratio, and the random variable b follows the Weibull distribution of 3 parameters. Through many studies and experiments, a rigid degradation model is proposed in this paper [30]. It is considered that under the condition of alternating load with constant stress amplitude, the residual stiffness can be expressed by the following formula:

$$\frac{E^*(n)}{n} = \frac{-a}{(n+1)E^*(n)^{m-1}}. \tag{19}$$

Based on the above equation, the stiffness decay rate equation under alternating fatigue load is obtained as follows:

$$F_{E(n)}(x) = 1 - \exp\left[-\left(\frac{(s/c)^{m/c} h \quad \ln(n+1)}{b^{m/c}(1 - x^m)}\right)^{ac/m}\right]. \tag{20}$$

After solving the parameters in the fatigue experimental equation, this paper improves the model and predicts the residual stiffness. When specific fragments are used to analyze the stress field and material properties of composites, they are affected by multiaxial fatigue load, providing an analysis method of stress field and residual stiffness degradation [31].

The stiffness attenuation of composites is affected by many external factors, such as stress level, laying method, material characteristics, and so on [32]. It is also the macro performance of internal damage under fatigue load, and can only represent the life span of materials, but it can not be accurately expressed [33]. Therefore, many researchers have obtained experimental results and put forward various macro phenomenon models to describe their attenuation law. However, this method is only applicable to specific materials [34].

3. Image Processing Experiment and Performance Analysis of Composite Fiber

3.1. Automatic Image Measurement of Fiber Length. The length distribution of short fibers in the matrix directly affects the mechanical properties of the composites. The strengthening effect can be brought into full play only when the fiber length is greater than the critical length. Therefore, it is very important to study the length distribution of fibers in composites. However, the current practice is usually to measure the fiber length by manually marking the fiber length on the fiber distribution image. Considering that the number of fibers measured usually exceeds hundreds, this measurement method is very inefficient. This chapter will propose an automatic fiber length measurement method to solve the above problems, in order to greatly improve the work efficiency and ensure the accuracy of the measurement results. In this paper, the mixture of carbon fiber and polylactic acid was prepared by an internal mixing process. The content of carbon fiber in the mixture was 15%. The carbon fiber reinforced polylactic acid composite spline was prepared by molding method.

This report analyzes carbon fiber-reinforced polylactic acid composites, so it is relatively simple and effective. The fibers in the composites were separated by the combustion method. Firstly, any part of the tested composite shall be cut

off, and then put into the furnace. Put the furnace into the furnace. In order to burn the plastic matrix, please burn it at 500°C for 4 hours. The separated carbon fibers are then cooled and randomly injected into the glass slide. Then drop a small amount of absolute ethanol on the glass slide, rotate back and forth on the glass slide to disperse the carbon fiber, and dry naturally in a windless place. Put the glass slide under the image measuring instrument for image acquisition to obtain the fiber length distribution diagram, as shown in Figure 5.

The fiber length distribution in the fiber distribution image above is calculated by the method in this paper. The calculation results are basically consistent with the manual calculation results, and the maximum comparison error is 5.4%. The fiber structure distribution is shown in Figure 6. Figure 6(a) is the fiber length distribution calculated manually, and Figure 6(b) is the fiber length distribution calculated automatically by this method.

In the above figure, the unit of fiber length is image pixel, and the actual length can be converted by scale. It can be seen that the method in this paper is very consistent with the manually calculated fiber length distribution, which shows that the method in this paper can well complete the measurement task of fiber length and its distribution under complex intersection conditions. In fact, the average error of all fiber lengths is only 6.7 pixels, and the maximum error is 21.4 pixels. The error is the largest when measuring the length of T-shaped cross fiber. This is because when calculating the length of one T-shaped cross fiber, the width of the other fiber will be considered, so the maximum error is close to the diameter of the fiber (about 18 pixels).

In order to further verify the effectiveness of the fiber orientation measurement method based on three-dimensional reconstruction of scanning electron microscope, the orientation of a single fiber in the cross-section of carbon fiber reinforced composite membrane was measured and compared with the results measured by image measuring instrument. In this paper, a low-content carbon fiber reinforced composite square film with a thickness of about 0.2 mm is used. The carbon fiber in the film is approximately two-dimensional oriented, so the deflection angle of the fiber can be measured by an image measuring instrument. Tilt the sample table to 5° and take SEM images of the fibers and the corresponding fibers pulled out of the cavity.

The deflection angle of a single fiber in five composite membranes was measured by two methods. The length of the fiber protruding from the matrix in the first to third membranes was larger, and the length of the fiber protruding from the matrix in the fourth and fifth membranes was smaller. The measurement results are shown in Table 1.

According to Table 1, the measurement results of this method are basically consistent with those of the image measuring instrument, with a maximum error of 1.4° and an average error of 0.83°. Usually, the information on fiber orientation angle only needs to obtain the proportion of fibers in a certain range, and the result of fiber orientation is not required to be very accurate. Therefore, this method can well measure the fiber orientation and distribution.

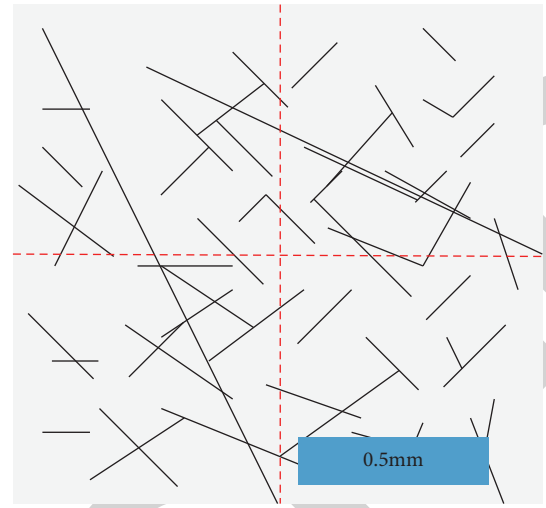

Figure 5: Fiber length distribution.

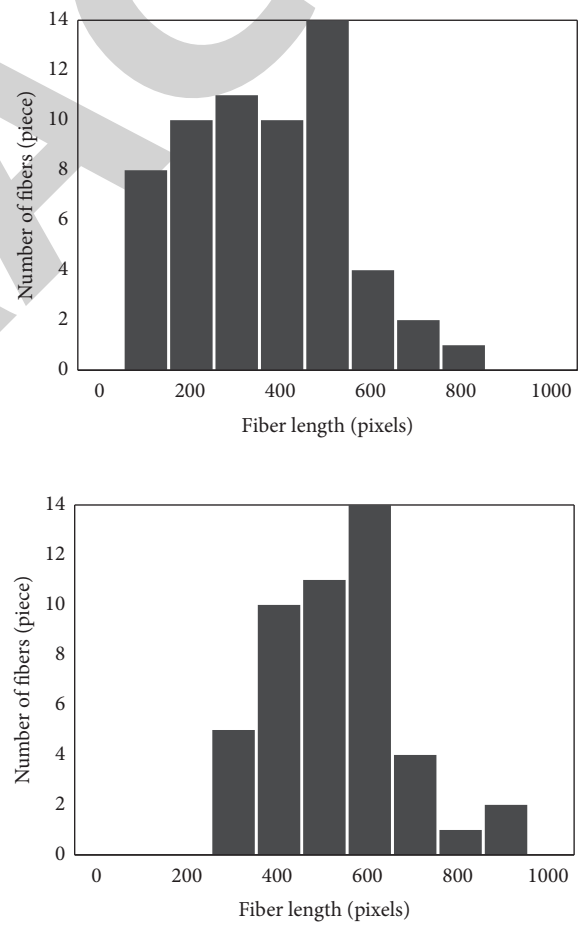

Figure 6: Fiber length distribution is obtained by different methods. (a) The result of manual calculation. (b) The result of applying the method in this paper.

The micromorphology of the composite section is very complex, and the actual orientation distribution of fibers in the material is also very complex. In some parts of the

Table 1: Measurement results of deflection angle of single fiber (°).

Serial number	Method of this article		Measuring instrument
	Fiber cavity	Fiber	
1	10.0	9.4	9.9
2	11.3	10.3	11.5
3	11.1	11.7	12.5
4	15.2	16.4	14.8
5	16.9	16.6	18.0

material, the fiber orientation may be in a relatively irregular state. At this time, the degree of fiber orientation cannot be judged by the naked eye alone. Figure 7 shows the results of measuring the deflection angle and azimuth of each fiber in the composite and the pull-out gap of the fiber by the method in this paper.

The reliability of the fiber orientation measurement method based on scanning electron microscope three-dimensional reconstruction technology is verified by experiments, and this method is applied to actual scanning electron microscope images. The results show that this method can well complete the task of measuring fiber orientation and distribution.

3.2. Study on Properties of Fiber Reinforced Composites. The performance test of fiber reinforced composites mainly includes mechanical performance tests (bending performance test, tensile performance test, impact performance test), contact angle test, microstructure test, thermodynamic performance test, processing flow performance test, DSC and POM test. The effect of fiber composite ratio on the mechanical properties of composites is recorded in Table 2.

It can be seen from the above table that when the ratio of composite fiber is 5:12:13, the mechanical properties of PP/EVA Composites are better. Among them, when the three fibers change from 5:20:5 to 5:16:9 and 5:12:13, the bending strength and tensile strength of the composite are greatly improved with the gradual increase of the proportion of fiber C. However, when the content of C fiber exceeds 13 parts, that is, when the ratio is 5:5:20, the mechanical properties of the composite are significantly reduced. On the contrary, when the ratio of the composite fiber changes from 5:5:50 to 5:16, and then to 5:12:13, the flexural strength of the composite increases with the increase of *X* fiber content. In order to optimize the system with better mechanical strength in this group of experiments, three composite ratios of RW: X: C = 5:12:13, 5:16:9 and 5:5:20 were selected to continue the exploration.

The hydrophilic contact angle on the surface of polypropylene/ethylene vinyl acetate composites reinforced by three modified fibers increases, which proves that the interfacial adhesion between fiber and resin is enhanced. Among them, with the increase of the proportion of fiber, the hydrophilic surface contact angle of the composite decreases, while with the increase of the proportion of SSIC fiber, the hydrophilic contact angle of the composite tends to

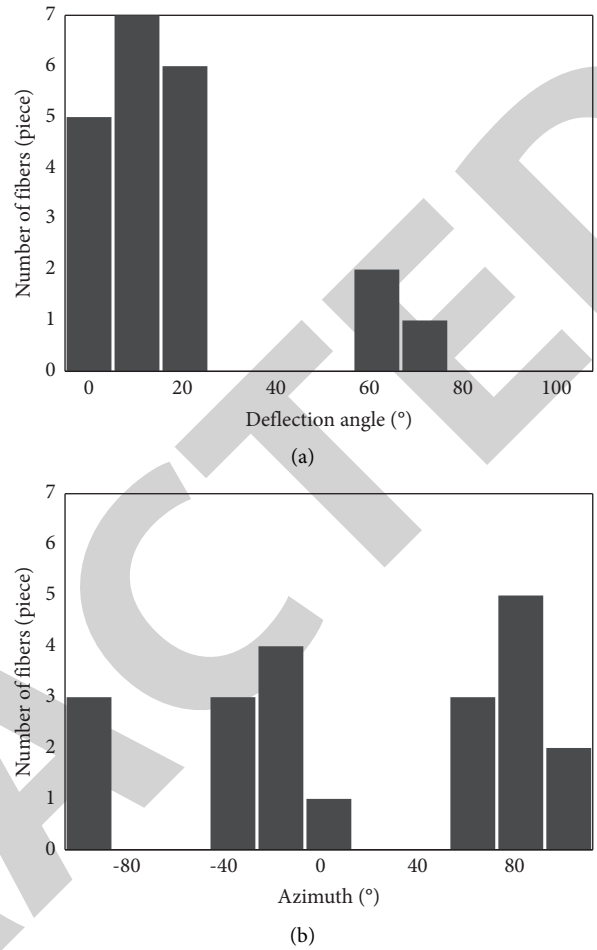

Figure 7: Corresponding fiber orientation distribution. (a) Deflection angle. (b) Azimuth.

Table 2: Effect of RW, *X*, and C fiber ratio on mechanical properties of composites.

RW:X:C	Tensile (MPa)	Flexural (MPa)	Impact (KJ/m^2)
5:12:13	22.36	38.79	5.78
5:16:9	24.66	35.01	6.17
5:9:16	24.79	35.69	5.84
5:20:5	23.28	36.64	5.96
5:5:20	24.48	34.68	5.55

Note. The amount of fiber is 30 parts, and the amount of PP/EVA is 70 parts, where PP:EVA = 4:1.

increase, which indicates that SSiX fiber is more hydrophilic than SSIC fiber. The surface hydrophilic contact angle of the composite is shown in Table 3.

The thermodynamic behavior analysis of three kinds of fiber-reinforced composites with changed properties increase the initial decomposition temperature, but the decomposition temperature increases with 50% weight loss, and the amount of residual carbon increases significantly. Moreover, the maximum decomposition rate is significantly lower than that of PP/EVA Composites. Therefore, increasing three different ratios of modified fiber is beneficial

Table 3: Surface hydrophilic contact angle of composites.

Composites	Different ratios	Average value of contact angle/°
PP/EVA/RW/SSIX/SSIC	5:5:20	86
	5:12:13	105
	5:16:9	90
PP/EVA/AW/SSIX/SSIC	5:5:20	94
	5:12:13	110
	5:16:9	80

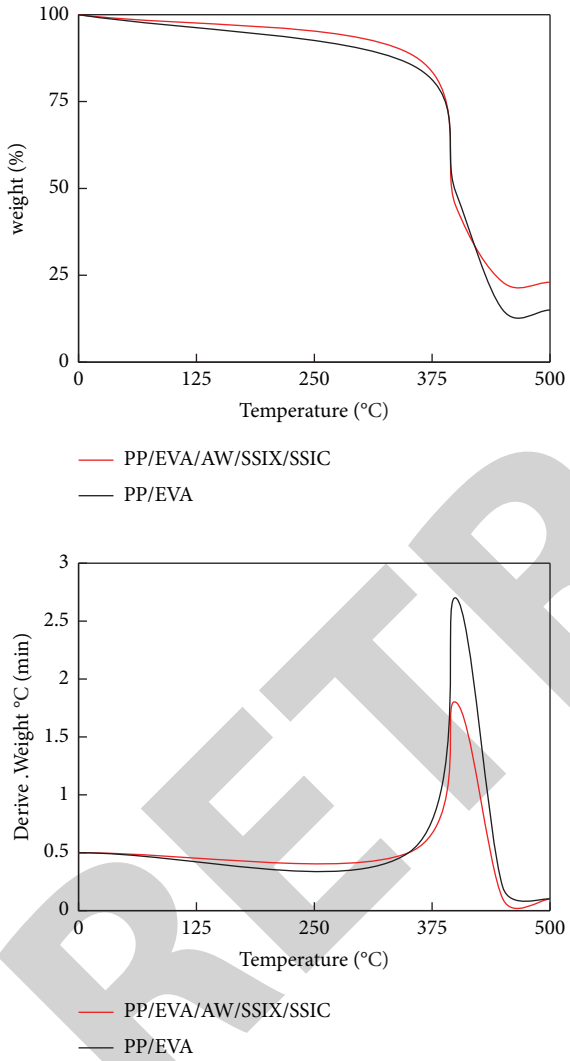

Figure 8: TG and DTG curves of three fiber composites.

to improve the thermal stability of polypropylene/ethylene vinyl acetate copolymer in high-temperature regions. Figure 8 shows the DTG and TG curves of a set of fiber composites.

In addition, it is not difficult to find in Table 4 that among the three ratios, when the ratio of SSiX fiber increases, the initial decomposition temperature of the composite increases significantly. At the same time, when the amount of SSIC fiber is large, the maximum decomposition rate decreases most obviously, and the amount of

Table 4: Thermogravimetric parameters of three fiber composites.

Composites	Td5% (°C)	Td50% (°C)	Vdmax (%/°C)	Yield at 550°C
PP/EVA	359.0	418.0	2.7	—
5:05:20	348.0	467.0	1.9	28.4
5:12:13	394.0	429.0	1.4	24.6
5:16:09	348.0	418.0	1.6	25.1

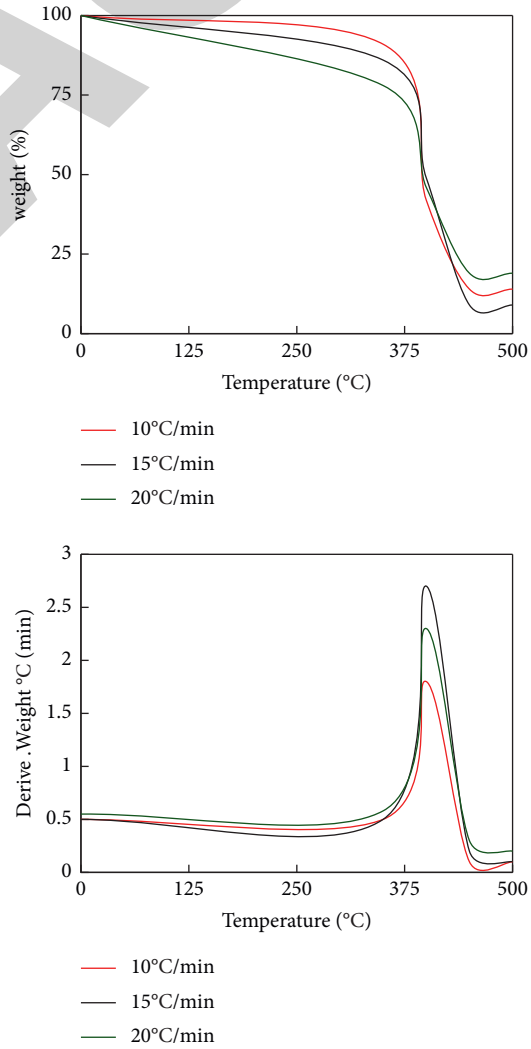

Figure 9: DTG and TG curves of composites at different heating rates.

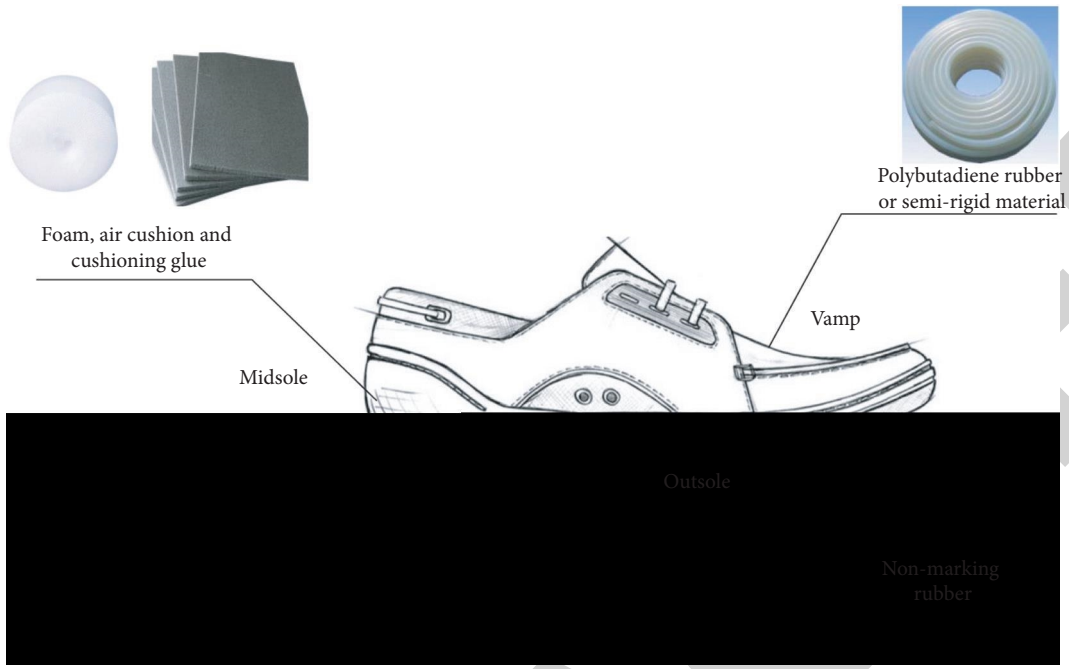

Figure 10: Structure of rubber shoes of new high-performance basketball shoes.

residual carbon is the largest, indicating that the basalt fiber plays a decisive role in the low-temperature thermal stability of the material. In composite materials, while carbon fiber enhances high-temperature thermal stability, the difference between the two fibers is very small.

As shown in Figure 9, under the same heating rate, the initial decomposition temperature Td5% of PP/EVA Composite with three modified composite fibers is faster than that of PP/EVA Composite. This is mainly due to the low-temperature decomposition of fibers. At different heating rates, the Tdmax of fiber PP/EVA Composites Modified by three compounds increases significantly with the increase of heating rate, mainly due to the delay of decomposition temperature of some substances due to accelerating heating rate, which is beneficial to the composites. At the same heating rate, the difference in Tdmax between the modified fiber and PP/EVA Composites is very small, but Tdmax tends to increase when the ratio of SSIC fiber increases. Compared with PP/EVA, the Vmax of all PP/EVA Composites added with three improved composite fibers was significantly reduced. When the mix ratio is aw: SSiX: SSiC = 5:5:20, the Vmax of the composite decreases to the minimum value of 1.35°C/min with the increase of heating speed, indicating that the thermal stability of the composite is improved.

3.3. Application Scenarios of Graphene Rubber. Liu Yuanshun proposed that athletes and coaches wear high-performance sports shoes to improve their sports performance. Most runners can run faster, about 1.6%. They can jump farther and reduce or reduce their injury probability. This theory can also be extended to basketball.

In theory, the components of shoes can improve athletes' jumping ability and reduce leg fatigue. The shoe parts with cushioning performance made of soft and high-energy feedback materials can get the maximum feedback value after being compressed by human feet. It can prevent foot injury and make athletes and other wearers feel comfortable.

On this basis, with the structure of the simplest rubber-based basketball shoes commonly used today and the use of graphene rubber composites, we can infer a new type of high-performance basketball shoes. The structural design and material use of the new basketball shoes are as follows: the first is the sole. Generally speaking, the outer layer of basketball shoes is made of unmarked rubber, and some manufacturers will add wear-resistant materials. Graphene natural rubber composites are used to exchange natural rubber with original colloids, and the excellent mechanical properties of graphene natural rubber composites are used to improve the tensile strength and tensile elastic modulus of colloids. The sole can have wrinkles. Moreover, it can not only prevent the soles from slipping, but also provide more energy feedback and cushioning. If force is applied to these products, wrinkles will be compressed, crushed, and absorb energy. When these forces are released, the antiwrinkle and rebound of the rubber sole can also provide more mechanical energy and elasticity. In addition, in order to protect the rubber base made of graphene natural rubber, a wear-resistant material layer can be sprayed on the outer surface of the rubber base. The second is the midsole. Generally speaking, the midsole of basketball shoes has cushion components such as cushion, cushion, cushion, and cushion. The insole or midsole of this new basketball shoe is laminated, including two layers of supporting materials (upper and lower). The top is covered with polybutadiene rubber or semirigid material to act as an additional layer or as a covering layer. In addition, it can also include two polybutadiene rubber layers. Each layer is about 80% CIs

polybutadiene rubber and about 20% natural rubber. It is a polybutadiene rubber layer with a thickness of about 7.9 MM, which is separated by the coating. The liner is more suitable for inserting into EVA/graphene natural rubber composite shoes. Figure 10 shows the structure of a new high-performance basketball shoe rubber material sneaker.

The new basketball shoes with graphene rubber can improve the fatigue strength and tensile strength of the shoes without increasing the overall weight of the shoes. The shoes contain 37.5% natural rubber, which can greatly prolong the service life, effectively solve the problem of shoe body deformation and strengthen the protection of athletes.

4. Discussion

In this paper, a fast edge extraction algorithm of OCT image based on phase consistency principle and morphological method is proposed, which proves the effectiveness of this algorithm. However, some work needs to be further improved. This paper only studies the fast image processing technology of swept frequency OCT systems from two aspects of image denoising and image edge extraction. In the imaging process of swept frequency OCT system, the process of signal preprocessing is essential. Therefore, we can deeply study the efficiency of signal preprocessing and find a more efficient preprocessing method. Based on the cylindrical characteristics of man-made fibers, in order to be applied to more complex reinforced fibers, such as plant fibers, it is necessary to further analyze the segmented combination rule of fiber skeleton in the length measurement method and the dense stereo matching algorithm in fiber orientation measurement method.

5. Conclusions

In this paper, the automatic fiber length measurement method based on the skeleton segment is used, and the obtained fiber length is basically consistent with the basic calculation value, and the maximum relative error is about 4.5%. The fiber length finally obtained is basically consistent with the theoretical calculation value. The average error is between 6.7 pixels and 21.4 pixels over each fiber length. This method can not only ensure accurate measurement of fiber length but also realize large-scale automated measurement. The fiber orientation was determined for the first time using the SEM reconstruction technique in the tests of fiber-reinforced composites and agreed with the results of the secondary imaging tests. The maximum deviations for the two methods are 3.83 and 1.54, respectively. (1) Through the experiment of graphene rubber application scenarios, the concept of user experience improvement is given. (2) By calculating the changes in user experience, we found that the comprehensive performance of sports products increased from 15.4% to 48.6% by using graphene rubber composite materials. (3) After using this material, its performance is improved by 2.1% to 4.5%. However, due to the limitation of time technology, this paper does not conduct in-depth research on fiber-reinforced composite materials, and we will further explore this in the follow-up.

Data Availability

This article does not cover data research. No data were used to support this study.

Conflicts of Interest

The author declares that there are no conflicts of interest.

References

[1] B. Jia and W. Zhang, "Application of digital image processing technology in online education under COVID-19 epidemic," *Journal of Intelligent and Fuzzy Systems*, no. 2, pp. 1–7, 2021.

[2] E. Oho, K. Suzuki, and S. Yamazaki, "Applying fast scanning method coupled with digital image processing technology as standard acquisition mode for scanning electron microscopy," *Scanning*, vol. 2020, no. 6, Article ID 4979431, 9 pages, 2020.

[3] X. Gu, H. Song, and J. Chen, "A review of research on pig behavior recognition based on image processing," *International Core Journal of Engineering*, vol. 6, no. 1, pp. 249–254, 2020.

[4] A. M. Elhousari, M. Rashad, A. H. Elsheikh, and M Dewidar, "The effect of rubber powder additives on mechanical properties of polypropylene glass-fiber-reinforced composite," *Mechanical Sciences*, vol. 12, no. 1, pp. 461–469, 2021.

[5] G. Yamamoto and T. Okabe, "Numerical study for tensile strength prediction of unidirectional carbon fiber-reinforced composite considering fiber surface stress concentration," *Mechanical Engineering Journal*, vol. 6, no. 3, pp. 19-00020-00020, 2019.

[6] S. Hamanaka, C. Nonomura, T. B. N. Thi, and A Yokoyama, "Correlation between fiber orientation distribution and mechanical anisotropy in glass-fiber-reinforced composite materials," *Journal of Polymer Engineering*, vol. 39, no. 7, pp. 653–660, 2019.

[7] S. T. Matsuwaka and E. W. Latzka, "Summer adaptive sports technology, equipment, and injuries," *Sports Medicine and Arthroscopy Review*, vol. 27, no. 2, pp. 48–55, 2019.

[8] Q. Feng and L. Wang, "The effect of polymer composite materials on the comfort of sports and fitness facilities," *Journal of Nanomaterials*, vol. 2022, Article ID 9108458, 2022.

[9] H. Jahangir, A. Soleymani, and M. R. Esfahani, "Investigating the confining effect of steel reinforced polymer and grout composites on compressive behavior of square concrete columns," *Iranian Journal of Science and Technology - Transactions of Civil Engineering*, 2022.

[10] F. Li, S. Zhang, and W. Cheng, "Application and optimization of wing structure design of DF-2 light sports aircraft based on composite material characteristics," *Journal of Nanomaterials*, vol. 2022, Article ID 6967016, 10 pages, 2022.

[11] A. Liu, H. Xie, and K. Ahmed, "Fault detection technology of national traditional sports equipment based on optical microscope imaging technology," *Alexandria Engineering Journal*, vol. 60, no. 2, pp. 2697–2705, 2021.

[12] L. Zhu, A. Wang, and F. Jin, "Using image processing technology and general fluid mechanics principles to model smoke diffusion in forest fires," *Fluid Dynamics & Materials Processing*, vol. 17, no. 5, pp. 1213–1222, 2021.

[13] D. G. Kim, K. J. Shin, and J. H. Woo, "Displacement measurement of steel pipe support using image processing technology," *Journal of Image and Graphics*, vol. 8, no. 3, pp. 80–84, 2020.

[14] Z. Gong, X. Li, and M. Ismail, "Automatic time attendance system based on intelligent image processing technology," *Journal of Intelligent and Fuzzy Systems*, no. 2, pp. 1–10, 2020.
[15] A. A. Elngar and S. E. El-Dek, "A novel artificial face mask based nanofibers with special intelligent engineered nanocomposite against covid-19," *Journal of Cybersecurity and Information Management*, vol. 5, no. 2, pp. 21-22, 2021.
[16] J. A. Eleiwy and N. Jaafar, "Novel filter of DWT for image processing applications," *Fusion: Practice and Applications*, vol. 4, no. 2, pp. 32–41, 2021.
[17] Y. Li, L. Chu, Y. Zhang, and C. Gao, "Intelligent transportation video tracking technology based on computer and image processing technology," *Journal of Intelligent and Fuzzy Systems*, vol. 37, no. 2, pp. 1–10, 2019.
[18] Y. Chen, X. Wu, J. Wei, and H Wu, "Characterization and application to fiber reinforced composite of catechol/polyethyleneimine modified polyester fabrics by mussel-inspiration," *Fibers and Polymers*, vol. 21, no. 11, pp. 2625–2634, 2020.
[19] K. Murali and D. V. Rama Koti Reddy, "Probability of detection analysis of frequency modulated thermal wave imaging to glass fiber–reinforced composite materials for nondestructive testing," *Journal of Testing and Evaluation*, vol. 48, no. 1, pp. 1–11, 2020.
[20] S. Yamur, A. Kurt, and U. Eker, "Evaluation and mathematical modeling of delamination and cutting forces in milling of carbon fiber reinforced composite (CFRP) materials," *Journal of the Faculty of Engineering and Architecture of Gazi University*, vol. 35, no. 1, pp. 457–465, 2020.
[21] S. H. Lee, S. H. Hwang, M. Kontopoulou et al., "The effect of physical treatments of waste rubber powder on the mechanical properties of the revulcanizate," *Journal of Applied Polymer Science*, vol. 112, no. 5, pp. 3048–3056, 2009.
[22] A. A. Khan, L. Perea-Lowery, and A. A. Al-Khureif, "Interfacial adhesion of a semi-interpenetrating polymer network-based fiber-reinforced composite with a high and low-gradient poly (methyl methacrylate) resin surface," *Polymers*, vol. 13, no. 352, pp. 1–9, 2021.
[23] D. Dennis, C. Hartanto, and W. Farahanny, "Comparative evaluation of short fiber-reinforced composite resin thickness on fracture resistance of class II composite restoration: an in vitro study," *The Journal of Contemporary Dental Practice*, vol. 21, no. 11, pp. 1201–1204, 2021.
[24] S. Kuchipudi, "NDE of Glass fiber reinforced composite structures using single sided solid state proton NMR," *Materials Today Proceedings*, vol. 21, no. 2, pp. 1239–1243, 2020.
[25] K. Sofiia, "Modernization of sports equipment as a factor of increasing of difficulty score of competitive routines in trampoline gymnastics," *Sport Science and Human Health*, vol. 4, no. 2, pp. 50–63, 2020.
[26] H. Zhu, H. Wei, B. Li, X. Yuan, and N. Kehtarnavaz, "Real-time moving object detection in high-resolution video sensing," *Sensors*, vol. 20, no. 12, p. 3591, 2020.
[27] G. H. Choi, H. Ko, W. Pedrycz, A. K. Singh, and S. B. Pan, "Recognition system using fusion normalization based on morphological features of post-exercise ecg for intelligent biometrics," *Sensors*, vol. 20, no. 24, p. 7130, 2020.
[28] e Montero, s kistamgari, t chounthirath, N. L. Michaels, M. Zhu, and G. A Smith, "Pediatric sports- and recreation-related dental injuries treated in US emergency departments," *Clinical Pediatrics*, vol. 58, no. 11-12, pp. 1262–1270, 2019.
[29] X. Liu and G. Ma, "Effects of nanomaterials on the body composition of patients with dyslipidemia based on different strength sports equipment," *Journal of Chemistry*, vol. 2020, no. 9, Article ID 3649157, 9 pages, 2020.
[30] J. W. . Winiewski, "Econometric forecasts of costs in a sports equipment trading enterprise," *Journal of Physical Education and Sport*, vol. 20, pp. 1092–1099, 2020.
[31] K. Ruan and Y. Li, "Fuzzy mathematics model of the industrial design of human adaptive sports equipment," *Journal of Intelligent and Fuzzy Systems*, vol. 40, no. 4, pp. 1–10, 2020.
[32] M. T. Nazeer, H. Atta, and A. Wahid, "Effects of parental involvement on the participation of students in sports," *Sir Syed Journal of Education & Social Research (SJESR)*, vol. 4, no. 1, pp. 440–447, 2021.
[33] J. E. Mencke, M. Salewski, O. L. Trinhammer, and A. T Adler, "Flight and bounce of spinning sports balls," *American Journal of Physics*, vol. 88, no. 11, pp. 934–947, 2020.
[34] C. L. Goh, "The challenge of regulating doping and non-doping "performance-enhancing strategies" in elite sports," *The International Sports Law Journal*, vol. 21, no. 1, pp. 47–61, 2021.